Two-dimensional rotation angle measurement using a sinusoidal phase-modulating laser diode interferometer

Osami Sasaki, MEMBER SPIE
Chikao Togashi
Takamasa Suzuki, MEMBER SPIE
Niigata University
Faculty of Engineering
Niigata-shi 950-2181, Japan
E-mail: osami@eng.niigata-u.ac.jp

Abstract. We propose a simple setup for measurement of a small 2-D rotation angle using a Twyman-Green laser diode interferometer. Sinusoidal phase-modulating interferometry is adopted to detect the phase of the interference signal with a high accuracy and to perform the phase lock to eliminate the phase fluctuation at the standard detection point. By detecting the phases at three points along an axis, the 1-D rotation angle is measured with an accuracy of 0.5 arcsec in the range of 282 arcsec and with a spatial resolution of 3 mm. The 2-D rotation angle measurement is easily made by adding two more detection points. © *2003 Society of Photo-Optical Instrumentation Engineers.* [DOI: 10.1117/1.1554407]

Subject terms: rotation angle measurement; interferometer; laser diode; phase lock.

Paper 020288 received Jul. 5, 2002; revised manuscript received Sep. 26, 2002; accepted for publication Oct. 2, 2002.

1 Introduction

The measurement of small rotation angles is necessary to fabricate precision mechanical and optical devices. Although autocollimators have been widely used for the measurement, they are rather large in structure and require a large reflection surface when a high accuracy is necessary. Setups using Michelson interferometers have been proposed for measurement of large rotation angles.[1–3] Right-angle prisms are placed on a measurement object to produce a change in the optical path difference according to the rotation angle. Since the phase change of the interference signal exceeds 2π for a large rotation angle, it is counted as many times as the phase changes by 2π while the object rotates. This measurement requires continuous detection of the phase. Setups using two beams polarized in two orthogonal directions and two rhomb prisms placed on a measurement object have the same characteristics as those using Michelson interferometer.[4,5] When a phase change is limited within 2π for small rotation angles, two phases detected before and after the object rotates provide the rotation angle. An instrument smaller in size than autocollimators is often requested that can measure a rotation angle smaller than several arcminutes with a spatial resolution less than about 3 mm and an accuracy higher than 1 arcsec. In this paper, we propose a setup using a Twyman-Green interferometer that satisfies the preceding measurement characteristics and achieves the 2-D measurement of small rotation angles. If we measure the rotation angle of a mirror attached to a measurement object or to the optical surface of the object itself, the setup becomes simple in structure and easy to handle.

For the small-angle measurement, other methods based on the internal reflection effect,[6] the fringe projection technique,[7,8] and the pattern projection technique[9] were reported. The method based on the internal reflection effect detects the intensity of reflected light, so that it is very sensitive to variations in the intensity of the light source and to stray light. The fringe projection technique is rather complicated in structure for 2-D measurement. The pattern projection technique involves a low spatial resolution.

Our proposed setup is a laser diode interferometer whose interference signal is sinusoidally phase modulated by modulating the injection current of the laser diode. The phase of the interference signal is detected accurately by sinusoidal phase-modulating interferometry.[10] Two values of the phase detected at two different points on a line perpendicular to the rotation axis of the object provide the inclination of a plane wave given by the rotation of the object surface. Mechanical vibrations or displacements of the optical components in the interferometer cause fluctuations in the phase of the interference signal. A phase detected at one measurement point is kept at a zero value by feedback control of the injection current to eliminate the phase fluctuations. This phase-lock operation is easily carried out in the sinusoidal phase-modulating interferometer.[11] Since the detection point where the phase is kept at a zero value is used as a standard detection point, the rotation angle can be easily obtained without phase unwrapping from the difference between the two values of the phase detected at the two points. In addition, a wide measurement range is achieved by adding one more detection point near the original detection point. If two more measurement points are added on a line perpendicular to the line where the three detection points have already been set, we can easily measure a 2-D rotation angle of a mirror surface with a Twyman-Green interferometer.

 0091-3286/2003/$15.00 © 2003 Society of Photo-Optical Instrumentation Engineers

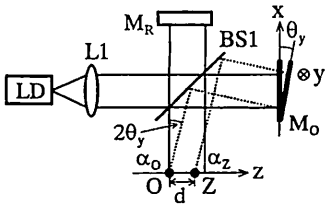

Fig. 1 Measurement of a 1-D rotation angle θ_y with a Twyman-Green interferometer.

2 Principle

2.1 *Basic Method*

We measure a 1-D rotation angle using a Twyman-Green interferometer, as shown in Fig. 1. The output light of a laser diode (LD) is collimated with lens L1 and divided into two waves with beamsplitter BS1. The two collimated waves are reflected by mirrors M_R and M_O, respectively. The two reflected waves are united with BS1 and produce an interferogram. Using this interferogram we measure rotation angle θ_y of mirror M_O, whose rotation axis is the y axis. The difference in propagation direction between the two reflected waves is $2\theta_y$. The phase of the interferogram is detected at two positions on the z axis, which is parallel to the surface of mirror M_R. The two position are indicated by O and Z, and the distance between O and Z is d. Denoting the phases at O and Z by α_O and α_Z, respectively, we have

$$\beta_Z = \alpha_Z - \alpha_O = (2\pi/\lambda) d \sin 2\theta_y, \tag{1}$$

where λ is wavelength of the light. When θ_y is very small, from Eq. (1) we obtain

$$\theta_y = (\lambda/4\pi d)\beta_Z. \tag{2}$$

Defining β_Z in the domain between $-\pi$ and π, the sign of β_Z represents the rotation direction. The size of the measurement range in θ_y is given by

$$S = \lambda/2d. \tag{3}$$

The measurement error in θ_y is in proportion to measurement error in β_Z, and it is in inverse proportion to d.

2.2 *Enlargement of Measurement Range*

Figure 2 shows a detection configuration by which we extend the measurement range in θ_y. Photodiode PD1 has two detection points indicated by $O1$ and $Z1$, which correspond to O and Z in Fig. 1, respectively. We obtain a measured value θ_{1y} from the two phases α_{O1} and α_{Z1} of the interferogram detected on $O1$ and $Z1$, respectively. Size S_1 of the measurement range in θ_{1y} is $\lambda/2d_1$. In addition, we use photodiode PD2, which has two detection points indicated by $O2$ and $Z2$. The reflected waves are divided with beamsplitter BS2 and the same interferogram as that on PD1 is enlarged by lenses L2 and L3 with magnification of $M = f_3/f_2$, where f_2 and f_3 are focal lengths of lenses L2 and L3, respectively. The light reaching $O2$ is almost the same as that at $O1$. The distance between positions $O2$ and $Z2$ is d_2', so that the distance between two measurement points on the interferogram detected with PD2 is $d_2 = (1/M)d_2'$ smaller than d_1. We obtain a measured value θ_{2y} from two phases α_{O2} and α_{Z2} of the interferogram detected at $O2$ and $Z2$, respectively. The measurement range of θ_{2y} is from $-\lambda/4d_2$ to $\lambda/4d_2$. Size S_2 of the measurement range in θ_{2y} is d_1/d_2 times as large as S_1 in θ_{1y}. While θ_{2y} increases from $-\lambda/4d_2$ to $\lambda/4d_2$, the measured value $\theta 1_y$ is distributed between $-\lambda/4d_1$ and $\lambda/4d_1$. The sign of θ_y is set to be the same as that of θ_{2y}. It is required that the value of θ_{1y} is converted into different range to be combined with the value of θ_{2y}. When θ_{2y} is positive, the value of θ_{1y} is converted into a range from 0 to $S_1 = \lambda/2d_1$ as follows:

$$\theta_{1y} = \begin{cases} \theta_{1y} - S_1 & \theta_{1y} \geq 0 \\ \theta_{1y} & \theta_{1y} < 0. \end{cases} \tag{4}$$

When θ_{2y} is negative, the value of θ_{1y} is converted into a range from 0 to $-\lambda/2d_1$ as follows:

$$\theta_{1y} = \begin{cases} \theta_{1y} & \theta_{1y} \leq 0 \\ \theta_{1y} + S_1 & \theta_{1y} < 0. \end{cases} \tag{5}$$

Using these converted values, rotation angle θ_y is given by

$$\theta_y = mS_1 + \theta_{1y}, \tag{6}$$

where m is an integer. A measured value of θ_{2y} is almost equal to θ_y given by Eq. (6). Substituting a measured value of θ_{2y} into θ_y and replacing m by m_c in Eq. (6), we have

$$m_c = (\theta_{2y} - \theta_{1y})/S_1. \tag{7}$$

If measurement error in θ_{2y} is smaller than $S_1/2$, an integer m is obtained by rounding off m_c. Thus we can obtain θ_y from the measured values of θ_{1y} and θ_{2y} with Eqs. (4) to (7). The sign of θ_y indicates the direction of the rotation. The limit of measurement range enlargement is determined by the condition that measurement error in θ_{2y} is smaller than $S_1/2$.

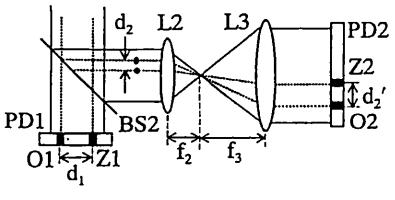

Fig. 2 Detection configuration to extend the measurement range.

2.3 *Two-Dimensional Measurement*

We use the four detection points of $O1$, $Z1$, $O2$, and $Z2$ to measure a rotation angle θ_y whose rotation axis is the y axis. A 2-D rotation angle has another component of θ_x besides θ_y. To measure rotation angle θ_x whose rotation axis is the x axis we add two detection points $Y1$ and $Y2$

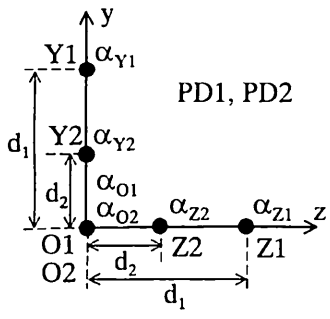

Fig. 3 Positions of the detection points and phases detected by PD1 and PD2.

located on the y axis direction, as shown in Fig. 3. Figure 3 shows positions of the detection points and detected phases. PD1 has three detecting points $O1$, $Z1$, and $Y1$ with an interval of d_1. PD2 has three detection points $O2$, $Z2$, and $Y2$ with an interval of d_2. Positions of $O1$ and $O2$ are located almost on the same point in the interferogram. Detected phases are denoted by variable α whose suffix means a detecting point. A rotation angle θ_x is obtained from $\alpha_{Y1}-\alpha_{O1}$ and $\alpha_{Y2}-\alpha_{O2}$ by the same method as θ_y.

3 Experimental Setup

Figure 4 shows a schematic of the experimental setup whose optical system contains the configurations shown in Figs. 1, 2, and 3. The conditions in the detection are as follows: $f_2=20$ mm, $f_3=70$ mm, $d_2=2/7$ mm, $d_2'=(f_3/f_2)d_2=1$ mm, and $d_1=3$ mm. We used a 2×2 elements photodiode as PD1 and PD2 on which three pinholes are set at the three positions shown in Fig. 3, respectively. We detect interference signals at six different positions. The injection current of the LD is modulated with a sinusoidal signal from an oscillator OSC to produce a sinusoidal phase-modulated interference signal. Phase of the interference signal is easily calculated with the sinusoidal-phase modulating interferometry. In addition we can obtain a signal of $\sin(\alpha_{O1})$ from the interference signal detected at position $O1$. This signal is fed to a feedback controller to control the injection current, and the feedback system keeps $\sin(\alpha_{O1})$ at zero value. This feedback control eliminates phase fluctuations on the standard detecting point and keeps

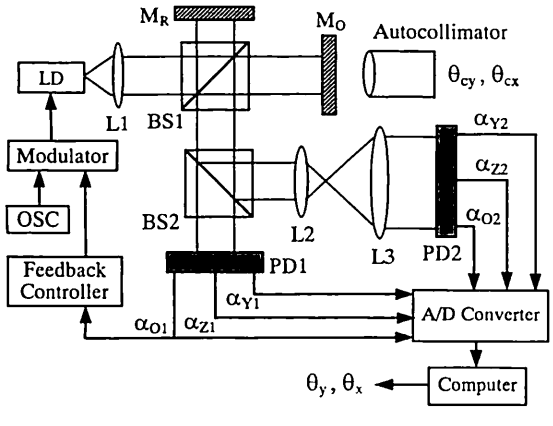

Fig. 4 Schematic of the experimental setup.

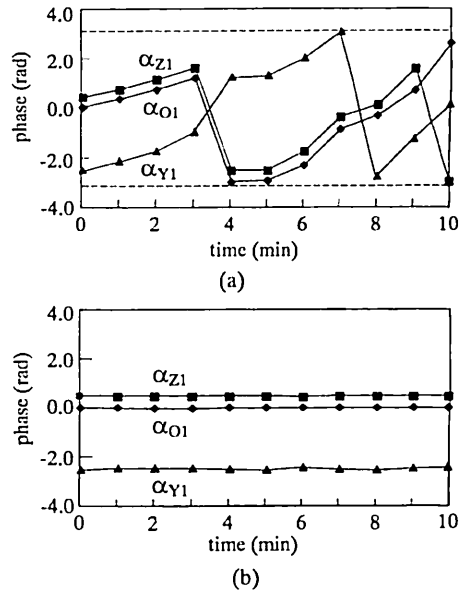

Fig. 5 Phase fluctuations (a) when the feedback control did not work and (b) when it worked for the phase α_{O1} to be kept at 0 rad.

α_{O1} and α_{O2} almost at zero radian. The six interference signals are analog-to-digital (A-D) converted to be fed to a computer. Six phases are calculated in the computer and finally the rotation angles θ_y and θ_x are obtained. The rotation angles are also measured with an autocollimator, and the measured values are denoted by θ_{cy} and θ_{cx}.

4 Experimental Result

First, we checked how much the phase fluctuations caused by mechanical vibrations are eliminated by the feedback control of the injection current of the LD. Since frequency of the sinusoidal phase-modulation was 2 kHz, the frequency bandwidth of the feedback control system was 200 Hz. Figure 5(a) shows the phase fluctuations in phases α_{O1}, α_{Z1}, and α_{Y1} when the feedback control did not work. Since the phases were wrapped in the region between $-\pi$ and π, it seems at first glance that the phase fluctuations were different from each other. If the unwrapping is done, it becomes clear that the phase fluctuations had almost the same increase with time. Therefore when the feedback control worked for phase α_{O1} to be kept at 0 rad, the phases α_{Z1} and α_{Y1} were also kept at constant values, as shown in Fig. 5(b). While the maximum deviation from a constant value in α_{O1} was about 0.01 rad, the maximum deviation in α_{Z1} and α_{Y1} was about 0.1 rad. These results indicate that the resolution in the sinusoidal phase-modulating interferometer was about 0.01 rad and the phase fluctuations in α_{Z1} and α_{Y1} were caused by the mechanical vibrations. These values of the deviations led to a measurement error of about 0.5 arcsec in θ_{1y} and θ_{1x}.

Second, we adjusted the rotational position of M_O so that β_{Z1} and β_{Y1} were almost equal to zero. At this rotational position, the measured values θ_{cy} and θ_{cx} of the autocollimator were set at zero value. After that we gave mirror M_O a rotation angle θ_y whose rotation axis was the y axis, and measured β_{Z1}, β_{Y1}, θ_{cy}, and θ_{cx}. The experi-

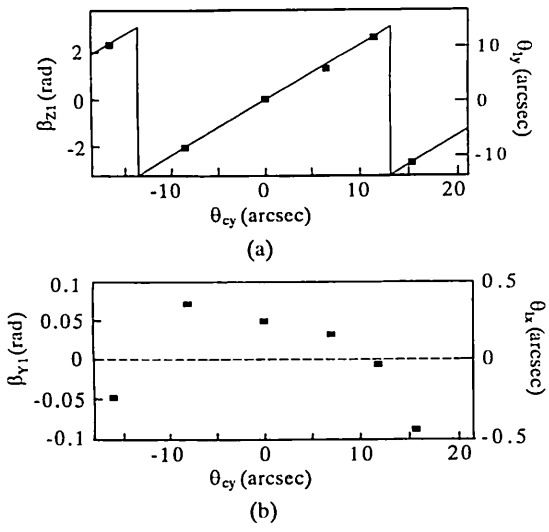

Fig. 6 Measured values of phases (a) β_{Z1} and (b) β_{Y1} for rotation angle θ_y.

mental results are shown in Fig. 6, where a measured value is indicated by a rectangular mark. In Fig. 6(a) the horizontal axis on the left side is β_{Z1}, and the corresponding value of θ_{1y} calculated with the relation of Eq. (2) is indicated along the horizontal axis on the right side, where λ was 779 nm. The solid line shows the theoretical relationship between β_{Z1} and θ_{cy} given by Eq. (2), in which θ_y, d, and β_Z are replaced by θ_{cy}, d_1, and β_{Z1}, respectively. From this result it became clear that measurement error in θ_{1y} was about 0.5 arcsec and the size of the measurement range in θ_{1y} agreed with the theoretical value of 26.8 arcsec obtained from the relation of Eq. (3). We also measured the rotation angle θ_{1x}, as shown in Fig. 6(b). Since the rotation axis of θ_y was the y axis, phase β_{Y1} was expected to be zero value. In practice, measured values of β_{Y1} were not zero and fluctuated. This fluctuation was caused by mechanical vibrations and was similar to that shown in Fig. 5(b).

Third, we set the measured values θ_{cy} and θ_{cx} of the autocollimator at zero when β_{Z1} and β_{Y1} were almost zero. After that we gave mirror M_O a rotation angle θ_y and measured θ_{cy}, θ_{cx}, β_{Z1}, β_{Z2}, β_{Y1}, and β_{Y2}. Results are

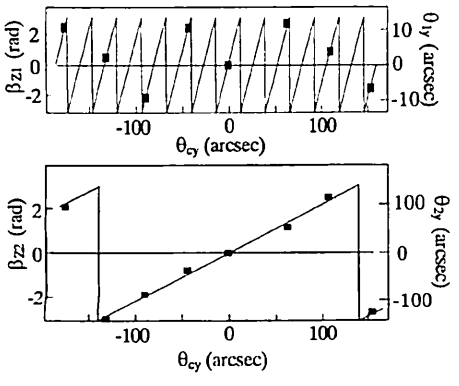

Fig. 7 Measured values of phases β_{Z1} and β_{Z2} for rotation angle θ_y.

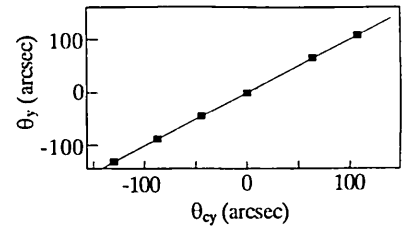

Fig. 8 Measured values of θ_y obtained from phases β_{Z1} and β_{Z2} for rotation angle θ_y.

shown in Fig. 7. The solid lines indicate the theoretical relationships between the rotation angle and the measured phase. Since the interval of the rotation angles was larger than the size of the measurement range in θ_{1y}, measured values of β_{Z1} were distributed discontinuously between $-\pi$ and π. Measurement error in θ_{1y} was always less than 0.5 arcsec, similar to that in Fig. 6(a). On the other hand, measured values of β_{Z2} changed continuously, corresponding to the rotation angle. Phase fluctuations in β_{Z2} were larger compared to β_{Z1} because phase α_{O2} was not exactly equal to phase α_{O1}. Measurement error in θ_{2y} was estimated to be less than about 10 arcsec from the result shown in Fig. 7. The size of the measurement range in θ_{2y} agreed with the theoretical value of 281.2 arcsec obtained from the relation of Eq. (3). To combine the two measured values of θ_{1y} and θ_{2y}, the measured values of θ_{1y} were converted into the different ranges with Eqs. (4) and (5) to obtain the value of m_c. The deviation in m_c from the corresponding integer was less than 0.3. This means that the measurement error in θ_{2y} was less than $S_1/2$, where S_1 was 26.8 arcsec. Measured values of θ_y obtained from Eq. (6) are shown in Fig. 8, where the measurement range was S_2 =281.2 arcsec and the measurement error was less than 0.5 arcsec. When we gave mirror M_O only a rotation angle θ_x whose rotation axis was the x axis, similar results were obtained for θ_{1x} and θ_{2x}. This result indicates that 2-D measurement is possible with the setup shown in Fig. 4.

Finally, we measured 2-D rotation angles of a mirror attached to a stage. After we adjusted the mirror at $\theta_x = \theta_y = 0$, we moved the stage in a direction of the z axis perpendicular to the mirror surface. We measured the rotation angles of θ_x and θ_y at four positions at intervals of 2 mm along the z axis. The result is shown in Fig. 9.

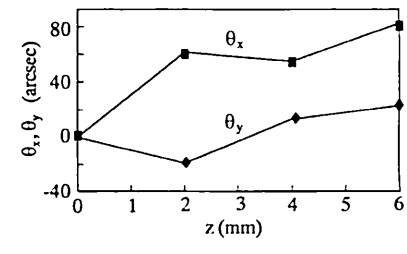

Fig. 9 Measurement result of 2-D rotation angles of a mirror attached to a stage.

5 Conclusion

We constructed a simple setup for the measurement of a small 2-D rotation angle using a Twyman-Green LD interferometer. Sinusoidal phase-modulating interferometry was adopted to detect the phase of the interference signal with a high accuracy and perform a phase lock to eliminate the phase fluctuation at the point of the standard detection point. By detecting the phases at three points along the axis we obtained measurement accuracy of 0.5 arcsec in the range of 282 arcsec with the spatial resolution of 3 mm for 1-D rotation angle. Two-dimensional rotation angle measurement was easily made by adding two more detection points.

References

1. P. Shi and E. Stijins, "New optical method for measuring small-angle rotations," *Appl. Opt.* **27**, 4342–4344 (1988).
2. P. Shi and E. Stijins, "Improving the linearity of the Michelson interferometric angular measurement by a parameter compensation method," *Appl. Opt.* **32**, 44–51 (1993).
3. M. Ikram and G. Hussain, "Michelson interferometer for precision angle measurement," *Appl. Opt.* **38**, 113–120 (1999).
4. M.-H. Chiu and D.-C. Su, "Angle measurement using total-internal reflection heterodyne interferometry," *Opt. Eng.* **36**, 1750–1753 (1997).
5. W. Zhou and L. Cai, "Improved angle interferometer based on total internal reflection," *Appl. Opt.* **38**, 1179–1185 (1999).
6. P. S. Huang and J. Ni, "Angle measurement based on the internal-reflection effect using elongated critical angle prisms," *Appl. Opt.* **35**, 2239–2241 (1996).
7. X. Dai, O. Sasaki, J. E. Greivenkamp, and T. Suzuki, "Measurement of two-dimensional small rotation angles by using orthogonal parallel interference patterns," *Appl. Opt.* **35**, 5657–5666 (1996).
8. X. Dai, O. Sasaki, J. E. Greivenkamp, and T. Suzuki, "High accuracy, wide range, rotation angle measurement by the use of two parallel interference patterns," *Appl. Opt.* **36**, 6190–6195 (1997).
9. T. Suzuki, H. Nakamura, O. Sasaki, and J. E. Greivenkamp, "Small-rotation-angle measurement using an imaging method," *Opt. Eng.* **40**, 426–432 (2001).
10. O. Sasaki and H. Okazaki, "Sinusoidal phase modulating interferometry for surface profile measurement," *Appl. Opt.* **25**, 3137–3140 (1986).
11. O. Sasaki, K. Takahashi, and T. Suzuki, "Sinusoidal phase modulating laser diode interferometer with a feedback control system to eliminate external disturbance," *Opt. Eng.* **29**(12), 1511–1515 (1990).

Biographies and photographs of the authors not available.